

Probing an emergent $U(1)$ extension of the Standard Model at colliders

Tran N. Hung* and Cao H. Nam†

*Phenikaa Institute for Advanced Study and Faculty of Fundamental Sciences,
Phenikaa University, Yen Nghia, Ha Dong, Hanoi 12116, Vietnam*

(Dated: March 22, 2023)

We explore the potential of probing for a new neutral gauge boson that emerges from a topologically nontrivial structure of spacetime, focusing on its couplings to the fermions of the Standard Model. We analyze the current experimental constraints on the mass of the new gauge boson and the radius of the fifth dimension, using the LEP bound and the LHC with 140 fb^{-1} luminosity. In addition, we investigate the indirect search of the new gauge boson and its discrimination from other hypothetical gauge bosons like those predicted in the $U(1)_{B-L}$ and $U(1)_R$ models by studying the forward-backward, left-right, and left-right-forward-backward asymmetries.

I. INTRODUCTION

Most of the elementary particle phenomena in the energy region below the TeV scale are successfully described by the Standard Model (SM) of particle physics which is based on the gauge symmetry $SU(3)_C \times SU(2)_L \times U(1)_Y$. In the SM, the right-handed neutrinos are absent and the neutrinos are massless. However, the measurements of the neutrino oscillation have provided solid evidence for the existence of the neutrino masses and flavor mixing [1–3]. This suggests that the SM has to be extended with new particles and interactions. A new $U(1)$ gauge symmetry, corresponding to a short-range Abelian gauge force, is a minimal extension of the SM and it is an active area at the LHC [4–10] and future colliders such as the International Linear Collider (ILC).

In the traditional way, the new $U(1)$ gauge symmetry is introduced through the extension of the SM gauge symmetry. Within this framework, the additional abelian gauge symmetry may be $B - L$ gauge symmetry [11–22], $B + L$ gauge symmetry [23, 24], $L_\mu - L_\tau$ gauge symmetry [25–37], or right-handed gauge symmetry [38–44]. The right-handed neutrinos are included for anomaly cancellations and carry non-zero charges under the additional $U(1)$ gauge symmetry. As a result, there are two possible mass types for the neutrinos, namely the Dirac type and the Majorana

*Electronic address: hung.tranngoc@phenikaa-uni.edu.vn

†Electronic address: nam.caohoang@phenikaa-uni.edu.vn

type, which could give a natural explanation for the light neutrino masses via the type-I seesaw mechanism. There, the Majorana masses of the right-handed neutrinos are related to the scale of the additional $U(1)$ gauge symmetry breaking.

However, we may ask ourselves whether the additional $U(1)$ gauge symmetry or the new Abelian gauge force may emerge from a nontrivial structure of spacetime. This question is motivated by the fact that the gravitational interaction arises from the nontrivial geometry of spacetime. In recent works [45, 46], we indicated the emergence of a new $U(1)_X$ gauge symmetry in the effective four-dimensional spacetime from the more fundamental five-dimensional spacetime which has a structure as follows: in general, the five-dimensional spacetime is only a local product of $\mathbb{R}^{3,1}$ and $U(1)$ rather than a global product. Due to the topological nontriviality of this structure of spacetime, a gauge field arises and transforms under the general coordinate change in the conventional Abelian gauge transformation. By considering the fields, which propagate dynamically in the five-dimensional spacetime and respect for the SM gauge symmetry, we obtained an emergent $U(1)_X$ extension of the SM in the effective four-dimensional spacetime, where the light neutrino masses are an unavoidable consequence of the structure of the spacetime. This scenario can solve two important issues of traditional Kaluza-Klein theories [47, 48] (also see Refs. [49, 50] for reviews): i) the right-handed and left-handed Weyl spinor fields as the representations of the Lorentz group $SO(3, 1)$ can be fundamentally defined in the five-dimensional spacetime due to the separation of the tangent (and cotangent) spaces of the five-dimensional spacetime into the horizontal and vertical subspaces without reference to the local coordinate system; ii) the SM fields carry non-zero charges under the emergent $U(1)_X$ gauge symmetry.

There are differences between the emergent $U(1)_X$ extension of the SM [45, 46] and the usual $U(1)$ extension of the SM. The first difference comes from the gauge charge assignment of the fields under the emergent $U(1)_X$ at which the right-handed neutrinos which are the zero modes do not carry charges under the emergent $U(1)_X$. The second difference is that the gauge coupling corresponding to the emergent $U(1)_X$ is completely determined by the difference between the mass of the zero modes and that of the corresponding KK excitation. The third difference is that there are unusual couplings of the new gauge boson to the KK excitations which have non-zero charges under the emergent $U(1)_X$.

The present work is organized as follows. In section II, we briefly review the emergent $U(1)_X$ extension of the SM. In section III, we investigate the collider constraints on the new gauge boson. We obtain the excluded parameter region using the LEP bound and current LHC limits on the production of the new gauge boson. In section IV, we consider the indirect search of the new gauge

boson and its discrimination from other hypothetical neutral gauge bosons by studying forward-backward, left-right, and left-right-forward-backward asymmetries. Finally, we conclude this work in section V. Note that, in the current work, we use units in $\hbar = c = 1$ and the signature of the metric as $(+, -, -, -, \cdots, -)$.

II. SETTINGS OF EMERGENT $U(1)_X$ SCENARIO

This section briefly reviews the emergent $U(1)_X$ extension of the SM arising from the topologically nontrivial structure of spacetime. For the details of this proposal, the readers see in Ref. [45].

A. Description of spacetime

Spacetime at a more fundamental level is assumed to be a five-dimensional fiber bundle M_5 , which is generally nontrivial, whose base manifold and fiber are $\mathbb{R}^{3,1}$ and the Lie group manifold $U(1)$, respectively. [Note that, in the case that the fiber bundle spacetime M_5 is trivial, M_5 would be a global product of $\mathbb{R}^{3,1}$ and $U(1)$.] In this sense, a local region of spacetime M_5 looks like a product $V_i \times U(1)$ where V_i is a local region of $\mathbb{R}^{3,1}$ [51]. Since the local coordinates for a point in spacetime M_5 are given by, $(x^\mu, e^{i\theta})$, where $\{x^\mu\} \in \mathbb{R}^{3,1}$ and $e^{i\theta} \in U(1)$ with θ to be dimensionless real parameter. The general coordinate transformation, which corresponds to the transition from one local coordinate system to another, is given by

$$\begin{aligned} x^\mu &\longrightarrow x'^\mu = x^\mu, \\ e^{i\theta} &\longrightarrow e^{i\theta'} = h(x)e^{i\theta}, \quad \text{or} \quad \theta \longrightarrow \theta' = \theta + \alpha(x). \end{aligned} \quad (1)$$

Let us present some critical properties of spacetime M_5 . The tangent space $T_p M_5$ at a point $p \in M_5$ is always decomposed into a direct sum of two subspaces without reference to the local coordinate system as [51]

$$T_p M_5 = H_p M_5 \oplus V_p M_5. \quad (2)$$

where $H_p M_5$ and $V_p M_5$ are four-dimensional horizontal tangent subspace and one-dimensional vertical subspace, respectively. The subspaces $H_p M_5$ and $V_p M_5$ are spanned by the covariant bases respectively given by

$$\left\{ \frac{\partial}{\partial x^\mu} - g_X X_\mu \frac{\partial}{\partial \theta} \equiv \hat{\partial}_\mu \right\}, \quad \frac{\partial}{\partial \theta} \equiv \partial_\theta, \quad (3)$$

where X_μ transforms under the general coordinate transformation (1) as

$$X_\mu \longrightarrow X'_\mu = X_\mu - \frac{1}{g_X} \partial_\mu \alpha(x), \quad (4)$$

and g_X is the gauge coupling. Note that, the gauge field X_μ would disappear in the case that the fiber bundle spacetime M_5 is trivial which means that M_5 is globally a direct product $\mathbb{R}^{3,1} \times U(1)$ because $T_p M_5 = T_x \mathbb{R}^{3,1} \oplus T_g U(1)$ with $x \in \mathbb{R}^{3,1}$ and $g \in U(1)$. Similarly, the cotangent space $T_p^* M_5$ which is dual to $T_p M_5$ is always decomposed into a direct sum of two subspaces without reference to the local coordinate system as

$$T_p^* M_5 = V_p^* M_5 \oplus H_p^* M_5, \quad (5)$$

where $H_p^* M_5$ and $V_p^* M_5$ are dual to $H_p M_5$ and $V_p M_5$, respectively. The dual subspaces $H_p^* M_5$ and $V_p^* M_5$ are spanned by the covariant bases $\{dx^\mu\}$ and $\{d\theta + g_X X_\mu dx^\mu\}$, respectively. With these natural decompositions, an inner product G on spacetime M_5 is defined as

$$G(V_1, V_2) = G_H(V_{1H}, V_{2H}) + G_V(V_{1V}, V_{2V}), \quad (6)$$

where V_{1H} (V_{2H}) and V_{1V} (V_{2V}) are the horizon and vertical components of the vector V_1 (V_2), respectively, the horizontal metric G_H is a tensor field belonging the space $H_p^* M_5 \otimes H_p^* M_5$ and given by

$$G_H = \eta_{\mu\nu} dx^\mu dx^\nu, \quad (7)$$

and the vertical metric G_V is a tensor field belonging the space $V_p^* M_5 \otimes V_p^* M_5$ and given by

$$G_V = -T^2(x, e^{i\theta}) \frac{(d\theta + g_X X_\mu dx^\mu)^2}{\Lambda^2}, \quad (8)$$

with the field $T(x, e^{i\theta})$ relating to the geometric size of the fiber and Λ to be a constant of the energy dimension. For simplicity, the theory is considered at the vacuum $\langle T(x, e^{i\theta}) \rangle = T_0$ and thus the geometric size of the fiber is fixed by the radius $R \equiv T_0/\Lambda$. One immediately checks that the following coordinate change

$$x^\mu \longrightarrow \Lambda^\mu{}_\nu x^\nu, \quad \theta \longrightarrow \theta, \quad (9)$$

with $\Lambda^\mu{}_\nu \in SO(3, 1)$ leaves invariant spacetime metric. Therefore, it is possible to define the usual right-handed and left-handed Weyl spinor fields in the fiber bundle spacetime M_5 , which does not happen to a general manifold.

B. A realistic model

Let us consider the fermion fields propagating in the fiber bundle spacetime M_5 and respecting the SM gauge symmetry. The fermion content is given by

$$\begin{aligned}
L_a(x, e^{i\theta}) &= \frac{1}{\sqrt{2\pi R}} \begin{pmatrix} \nu_{aL}(x) \\ e_{aL}(x) \end{pmatrix} e^{iX_L\theta} \equiv \frac{L_a(x)}{\sqrt{2\pi R}} e^{iX_L\theta} \sim \left(1, 2, -\frac{1}{2}\right), \\
E_{aR}(x, e^{i\theta}) &= \frac{e_{aR}(x)}{\sqrt{2\pi R}} e^{iX_E\theta} \sim (1, 1, -1), \\
N_{aR}(x, e^{i\theta}) &\sim (1, 1, 0), \\
Q_a(x, e^{i\theta}) &= \frac{1}{\sqrt{2\pi R}} \begin{pmatrix} u_{aL}(x) \\ d_{aL}(x) \end{pmatrix} e^{iX_Q\theta} \equiv \frac{Q_a(x)}{\sqrt{2\pi R}} e^{iX_Q\theta} \sim \left(3, 2, \frac{1}{6}\right), \\
D_{aR}(x, e^{i\theta}) &= \frac{d_{aR}(x)}{\sqrt{2\pi R}} e^{iX_D\theta} \sim \left(3, 1, -\frac{1}{3}\right), \\
U_{aR}(x, e^{i\theta}) &= \frac{u_{aR}(x)}{\sqrt{2\pi R}} e^{iX_U\theta} \sim \left(3, 1, \frac{2}{3}\right), \tag{10}
\end{aligned}$$

where the numbers given in parentheses refer to the gauge charge assignment under the SM gauge symmetry. We can see that, except the right-handed neutrinos N_{aR} , all bulk fields $\{L_a, E_a, Q_a, D_a, U_a\}$ carry the corresponding numbers $\{X_L, X_E, X_Q, X_D, X_U\}$ which characterize the $U(1)$ active action on these fields. As indicated in Ref. [45], this is because the vertical “kinetic” term of these fields is forbidden by the SM gauge symmetry. And, thus the θ -dependence of these fields is not determined unless they are invariant under the $U(1)$ active action. In addition, as seen later, the fields $\{L_a(x), e_{aR}(x), Q_a(x), d_{aR}(x), u_{aR}(x)\}$ are identified as the SM fermion fields. Under the general coordinate transformation (1), we have $F'(x', e^{i\theta'}) = F(x, e^{i\theta})$, with F referring to the bulk fields $\{L_a, E_a, Q_a, D_a, U_a\}$, which suggests the following transformation

$$f(x) \longrightarrow f'(x) = e^{-iX_F\alpha(x)} f(x), \tag{11}$$

where $f(x)$ refers to $\{L_a(x), E_a(x), Q_a(x), D_a(x), U_a(x)\}$. The transformation (11) is nothing but the $U(1)_X$ local gauge transformation for the matter fields.

From (10), one can see that the transforming parameters of the SM gauge symmetry are completely independent of the fiber coordinate θ . This thus leads to the simplest form for the gauge fields of the SM gauge symmetry as

$$\begin{aligned} G_{aM} &= \left(\frac{G_{a\mu}(x)}{\sqrt{2\pi R}}, 0 \right), \\ W_{iM} &= \left(\frac{W_{i\mu}(x)}{\sqrt{2\pi R}}, 0 \right), \\ B_M &= \left(\frac{B_\mu(x)}{\sqrt{2\pi R}}, 0 \right), \end{aligned} \quad (12)$$

where their vertical component is zero.

Let us write bulk action for the gauge bosons and fermions (with the gauge fixing and ghost terms dropped) as

$$\begin{aligned} S_{\text{FG}}^{\text{bulk}} &= \int d^4x d\theta \sqrt{|\det G|} \left(\mathcal{L}_{\text{gauge}}^{\text{bulk}} + \mathcal{L}_{\text{fer}}^{\text{bulk}} \right), \\ \mathcal{L}_{\text{gauge}}^{\text{bulk}} &= -\frac{1}{4} G_{aMN} G_a^{MN} - \frac{1}{4} W_{iMN} W_i^{MN} - \frac{1}{4} B_{MN} B^{MN} + \frac{M_*^3}{2} \mathcal{R}, \\ \mathcal{L}_{\text{fer}}^{\text{bulk}} &= \sum_F \bar{F} i \gamma^\mu \hat{D}_\mu F + \bar{N}_{aR} i \gamma^\mu \hat{\partial}_\mu N_{aR} + \frac{1}{2\Lambda} \left(\partial^\theta \bar{N}_{aR}^C \partial_\theta N_{aR} - M_{N_a}^2 \bar{N}_{aR}^C N_{aR} + \text{H.c.} \right), \end{aligned} \quad (13)$$

where

$$\begin{aligned} G_{a\mu\nu} &= \partial_\mu G_{a\nu} - \partial_\nu G_{a\mu} + g_s f_{abc} A_{b\mu} A_{c\nu}, \\ W_{i\mu\nu} &= \partial_\mu W_{i\nu} - \partial_\nu W_{i\mu} + g \varepsilon_{ijk} W_{j\mu} W_{k\nu}, \\ B_{\mu\nu} &= \partial_\mu B_\nu - \partial_\nu B_\mu, \end{aligned} \quad (14)$$

are the field strength tensors (up to a normalized factor) corresponding to the gauge groups $SU(3)_C$, $SU(2)_L$, and $U(1)_Y$, respectively, \mathcal{R} is the scalar curvature of spacetime M_5 , M_* is the five-dimensional Planck scale related to the four-dimensional one M_{Pl} as, $2\pi R M_*^3 = M_{\text{Pl}}^2$, M_{N_a} are the vertical “mass” parameters of the right-handed neutrinos N_{aR} , and the covariant derivative \hat{D}_μ reads

$$\hat{D}_\mu = \partial_\mu - i g_s \frac{\lambda^a}{2} G_{a\mu} - i g \frac{\sigma^i}{2} W_{i\mu} - i g' Y_F B_\mu, \quad (15)$$

with $\{g_s, g, g'\}$ to be the gauge couplings corresponding to $\{SU(3)_C, SU(2)_L, U(1)_Y\}$, respectively. (Note that, the scalar sector and Yukawa couplings, which play no role in this work, are discussed in Ref. [45].) Then, one can find the effective four-dimensional action as

$$S_{\text{FG}}^{\text{eff}} = \int d^4x \left(\sum_f \bar{f} i \gamma^\mu D_\mu f + \mathcal{L}_N - \frac{1}{4} G_{a\mu\nu} G^{a\mu\nu} - \frac{1}{4} W_{i\mu\nu} W^{i\mu\nu} - \frac{1}{4} B_{\mu\nu} B^{\mu\nu} - \frac{1}{4} X_{\mu\nu} X^{\mu\nu} \right),$$

$$\begin{aligned}
\mathcal{L}_N &= \mathcal{L}_\nu + \mathcal{L}_\psi + \mathcal{L}_\chi + \mathcal{L}_{\text{int}}, \\
\mathcal{L}_\nu &= \bar{\nu}_{aR} i \gamma^\mu \partial_\mu \nu_{aR} - \frac{M_{a0}}{2} \bar{\nu}_{aR}^C \nu_{aR} + \text{H.c.}, \\
\mathcal{L}_\psi &= \sum_{n=1}^{\infty} \left(\bar{\psi}_{naR} i \gamma^\mu \partial_\mu \psi_{naR} - \frac{M_{an}}{2} \bar{\psi}_{naR}^C \psi_{naR} + \text{H.c.} \right), \\
\mathcal{L}_\chi &= \sum_{n=1}^{\infty} \left(\bar{\chi}_{naR} i \gamma^\mu \partial_\mu \chi_{naR} - \frac{M_{an}}{2} \bar{\chi}_{naR}^C \chi_{naR} + \text{H.c.} \right), \\
\mathcal{L}_{\text{int}} &= i g_X \sum_{n=1}^{\infty} n \left(\bar{\chi}_{naR} \gamma^\mu \psi_{naR} - \bar{\psi}_{naR} \gamma^\mu \chi_{naR} \right) X_\mu,
\end{aligned} \tag{16}$$

where the covariant derivative D_μ is given by

$$D_\mu = \partial_\mu - i g_s \frac{\lambda^a}{2} G_{a\mu} - i g \frac{\sigma^i}{2} W_{i\mu} - i g' Y_f B_\mu - i g_X X_f X_\mu, \tag{17}$$

$\nu_{aR}(x)$ are identified as the usual right-handed neutrinos and $\{\psi_{naR}, \chi_{naR}\}$ are their Kaluza-Klein (KK) excitations whose masses are given by

$$\begin{aligned}
M_{a0} &= \frac{M_{N_a}^2}{\Lambda}, \\
M_{an} &= \frac{1}{\Lambda} \left(M_{N_a}^2 + \frac{n^2}{R^2} \right),
\end{aligned} \tag{18}$$

and $X_{\mu\nu} = \partial_\mu X_\nu - \partial_\nu X_\mu$ is the field strength tensor of X_μ . Note that, for a convenient reason we have replaced Y_F and X_F with Y_f and X_f , respectively.

From the effective action (16), we see that a gauge symmetry $U(1)_X$ emerges in the effective four-dimensional spacetime, which originates from the more fundamental five-dimensional spacetime. The charges of the SM fermions under the emergent symmetry $U(1)_X$ are the quantum numbers characterizing the $U(1)$ active action on them. The usual right-handed neutrinos ν_{aR} have no charge under $U(1)_X$, which is different from the usual $U(1)$ extension of the SM in which the right-handed neutrinos carry non-zero charges under an additional $U(1)$. Whereas, their KK excitations $\{\psi_{naR}, \chi_{naR}\}$ carry non-zero $U(1)_X$ charges but their couplings to the X gauge boson are unusual. By requiring the emergent $U(1)_X$ gauge symmetry to be free anomaly, we can determine the $U(1)_X$ charges of the SM fermions given in Table I.

Fermion f	ν_{aL}	e_{aL}	e_{aR}	u_{aL}	d_{aL}	u_{aR}	d_{aR}
X_f	$-x$	$-x$	$-2x$	$\frac{1}{3}x$	$\frac{1}{3}x$	$\frac{4}{3}x$	$-\frac{2}{3}x$

TABLE I: The $U(1)_X$ charges of the SM fermions with x to be a free parameter which is set to be 1 in this work.

It is important to mention that the gauge coupling g_X associated with the emergent symmetry $U(1)_X$ is determined in terms of the radius R of the fiber and the reduced four-dimensional Planck scale M_{Pl} as

$$g_X = \frac{\sqrt{2}}{M_{\text{Pl}} R}. \quad (19)$$

This relation suggests that if $R^{-1} \ll M_{\text{Pl}}$ the gauge coupling g_X is very small. For example, the inverse radius of the fiber is in order of the GUT scale, 10^{15} GeV, then the gauge coupling g_X is about 10^{-3} . Of course, the gauge coupling g_X is possibly below the order 10^{-3} if the inverse radius of the fiber is smaller than the GUT scale. Therefore, even the spontaneous breaking scale of the symmetry group $U(1)_X$ is much bigger than the electroweak scale, and the X gauge boson mass is either a few TeV or lighter. Because of its small coupling strength, the X gauge boson has evaded detection at the LHC as well as the indirect searches at other colliders. However, the X gauge boson can be observed for the high enough integrated luminosity such as $\mathcal{L} = 3000$ fb $^{-1}$ corresponding to the high-luminosity LHC (HL-LHC). Assessing the direct/indirect discovery potential for the X gauge boson at the colliders is subject to the investigation in the following section.

III. COLLIDER CONSTRAINT ON X GAUGE BOSON

In this section, we study the constraints on the X gauge boson from the present collider data, focusing on its couplings to the SM fermions.

A. Constraint from the LEP

The X gauge boson would contribute to the scattering process $e^+e^- \rightarrow f^+f^-$ and thus should lead to the deviations from the SM prediction in this scattering process. Contact interactions between electrons and fermions (charged leptons or quarks) can be parametrized by the following effective Lagrangian

$$\begin{aligned} \mathcal{L}_{\text{eff}} &= \frac{1}{1 + \delta_{ef}} \frac{g_X^2}{M_X^2} [X_{e,L} \bar{e}_L \gamma_\mu e_L + X_{e,R} \bar{e}_R \gamma_\mu e_R] [X_{f,L} \bar{f}_L \gamma^\mu f_L + X_{f,R} \bar{f}_R \gamma^\mu f_R], \\ &= \frac{1}{1 + \delta_{ef}} \frac{g_X^2}{M_X^2} \sum_{i,j=L,R} \eta_{ij} \bar{e}_i \gamma_\mu e_i \bar{f}_j \gamma^\mu f_j, \end{aligned} \quad (20)$$

where $\delta_{ef} = 1(0)$ for $f = e$ ($f \neq e$), and $\eta_{ij} = X_{e,i}X_{f,j}$. The LEP data given in Ref. [52] imposes the following constraint

$$\frac{2\sqrt{\pi}M_X}{\sqrt{C_{e,V}^2 + C_{e,A}^2}} \gtrsim 24.6 \text{ TeV}, \quad (21)$$

which leads to a lower bound on the ratio of the X gauge boson mass M_X to the inverse radius of the fiber as

$$\frac{M_X}{R^{-1}} \gtrsim 6.4 \times 10^{-15}. \quad (22)$$

Note that, the universality in the couplings of the X gauge boson to the charged leptons has been used and the $U(1)_X$ charges of the charged leptons are to correspond to model VV^+ in Ref. [52].

B. Constraint from the LHC

The production and decays of the X gauge boson at the LHC are through the most promising channel, namely the Drell-Yan process $pp \rightarrow \gamma, Z, X \rightarrow l^+l^-$ ($l = e, \mu$). The cross-section distribution for this process can be written, with no cut on the lepton pair rapidity, as

$$\begin{aligned} \frac{d\sigma}{d\hat{s}} &= \sum_q L_{q\bar{q}}(\hat{s}) d\hat{\sigma}(q\bar{q} \rightarrow \gamma, Z, X \rightarrow l^+l^-), \\ &= \frac{\hat{s}}{72\pi} \sum_q L_{q\bar{q}}(\hat{s}) \sum_{i,j \geq i} \frac{P_{ij}}{1 + \delta_{ij}} C_S^{ij}, \end{aligned} \quad (23)$$

where $\sqrt{\hat{s}}$ is the invariant mass of the dilepton system, $i, j = (\gamma, Z, X)$, P_{ij} are functions of the mass and the total width of the gauge bosons involved in the process given by [53]

$$P_{ij} = \frac{(\hat{s} - M_i^2)(\hat{s} - M_j^2) + M_i M_i \Gamma_i \Gamma_j}{\left[(\hat{s} - M_i^2)^2 + M_i^2 \Gamma_i^2\right] \left[(\hat{s} - M_j^2)^2 + M_j^2 \Gamma_j^2\right]}, \quad (24)$$

the symmetric coefficient C_S^{ij} is defined as [53]

$$C_S^{ij} = \left(C_{q,L}^i C_{q,L}^j + C_{q,R}^i C_{q,R}^j\right) \left(C_{l,L}^i C_{l,L}^j + C_{l,R}^i C_{l,R}^j\right), \quad (25)$$

and $L_{q\bar{q}}$ is the parton luminosities defined by

$$L_{q\bar{q}}(\hat{s}) = \int_{\frac{\hat{s}}{s}}^1 \frac{dx}{xs} \left[f_q(x, \hat{s}) f_{\bar{q}}\left(\frac{\hat{s}}{xs}, \hat{s}\right) + f_q\left(\frac{\hat{s}}{xs}, \hat{s}\right) f_{\bar{q}}(x, \hat{s}) \right], \quad (26)$$

with \sqrt{s} to be a fixed collider center-of-mass energy and $f_{q(\bar{q})}(x, \hat{s})$ to be the parton distribution function (PDFs) of the quark q (antiquark \bar{q}) evaluated at the scale \hat{s} [54]. The total cross section for this process is obtained by, $\int_0^s d\hat{s} \frac{d\sigma}{d\hat{s}}$.

Let us obtain the constraint on the mass and the gauge coupling of the X gauge boson from the negative signal for the dilepton resonances at the LHC. In order to do this, we compare the cross-section for the subprocess $pp \rightarrow X \rightarrow l^+l^-$ and the 95% confidence level (CL) upper limits on $\sigma \times BR$ of new neutral gauge boson (which have been produced under the assumption of a narrow neutral gauge boson resonance) using the LHC at $\sqrt{s} = 13$ TeV with 140 fb^{-1} luminosity [55, 56]. Hence, first we write the cross-section for the subprocess $pp \rightarrow X \rightarrow l^+l^-$ from (23) after subtracting the SM background and the interference effects between the X gauge boson and the SM neutral gauge bosons, in the narrow width approximation as

$$\sigma(pp \rightarrow X \rightarrow l^+l^-) = \frac{\pi}{6} \sum_q L_{q\bar{q}}(M_X^2) (C_{q,L}^2 + C_{q,R}^2) \text{Br}(X \rightarrow l^+l^-), \quad (27)$$

where $\text{Br}(X \rightarrow l^+l^-)$ is the branching ratio of the X gauge boson decay into the given lepton-antilepton pair l^+l^- given by [45]

$$\text{Br}(X \rightarrow l^+l^-) = \frac{\Gamma(X \rightarrow l^+l^-)}{\Gamma_X} \approx 12.5\%.$$

Note that, for the tree-level decays into the two-body final states, in our scenario the X gauge boson decay into the SM fermion pairs only [45], which means that the total decay width of the X gauge boson is given as $\Gamma_X = \sum_f \Gamma(X \rightarrow f\bar{f})$ where

$$\Gamma(X \rightarrow f\bar{f}) = \frac{N_C(f)M_X}{24\pi} g_X^2 \sqrt{1 - \frac{4m_f^2}{M_X^2}} \left[(X_{f_L}^2 + X_{f_R}^2) \left(1 - \frac{m_f^2}{M_X^2} \right) + 6X_{f_L}X_{f_R} \frac{m_f^2}{M_X^2} \right], \quad (28)$$

with $N_C(f)$ being the color number of the fermion f .

With the 95% CL upper limits on $\sigma \times BR$ of new neutral gauge boson from the LHC at $\sqrt{s} = 13$ TeV with 140 fb^{-1} luminosity [55, 56], we show the upper bound curve in the $M_X - R^{-1}/M_{\text{Pl}}$ plane as the black solid curve in Fig. 1. In addition, we combine the LEP bound that is given by Eq. (22) and the dashed black line in Fig. 1 to obtain the excluded region of the emergent $U(1)$ gauge boson mass and the radius of the fiber S^1 . The region above the dashed black line is excluded by the LEP bound, whereas the region above the black solid curve is excluded by the current LHC limits on the production of the new neutral gauge boson. According to this figure, the direct search of the new neutral gauge boson at the LHC imposes the most stringent bound on the relation between the new X gauge boson mass and the inverse radius of the fiber.

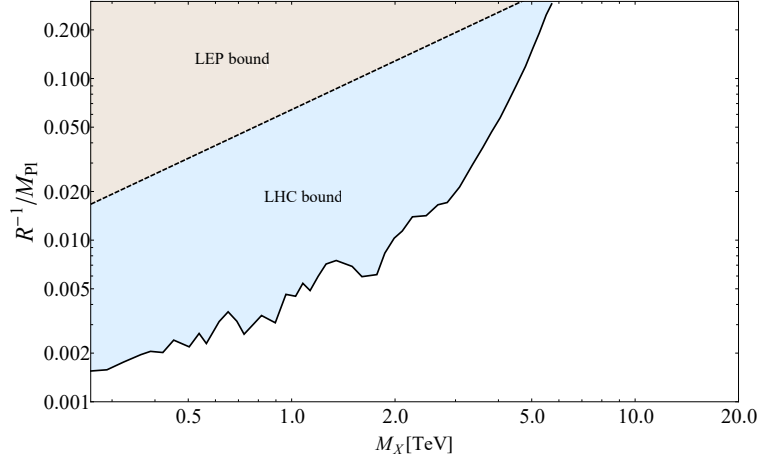


FIG. 1: The allowed parameter region (white region) in the $M_X - R^{-1}/M_{\text{Pl}}$ plane from the combination of the LEP and current LHC constraints.

IV. X BOSON SEARCH THROUGH ASYMMETRIES

A. Forward-backward asymmetry

At the ILC, the final state $\mu^+\mu^-$ is the most sensitive mode, since we focus on the following process

$$e^-(k_1, \sigma_1) + e^+(k_2, \sigma_2) \rightarrow \mu^-(k_3, \sigma_3) + \mu^+(k_4, \sigma_4), \quad (29)$$

where $\sigma_i = \pm 1$ and k_i are the helicities and the 4-momentum of the leptons, respectively. The helicity amplitudes of this process coming from the s -channel γ , Z , and X exchanges are given by

$$\begin{aligned} \mathcal{M}(+-+-) &= -4\pi\alpha(1 + \cos\theta)s \left[\frac{1}{s} + \frac{c_R^2}{s_Z} + \frac{C_{e,R}^2}{4\pi\alpha s_X} \right], \\ \mathcal{M}(-+-+) &= -4\pi\alpha(1 + \cos\theta)s \left[\frac{1}{s} + \frac{c_L^2}{s_Z} + \frac{C_{e,L}^2}{4\pi\alpha s_X} \right], \\ \mathcal{M}+--+) &= \mathcal{M}(-++-) = 4\pi\alpha(1 - \cos\theta)s \left[\frac{1}{s} + \frac{c_R c_L}{s_Z} + \frac{C_{e,R} C_{e,L}}{4\pi\alpha s_X} \right], \\ \mathcal{M}(++++ &= \mathcal{M}(----) = 0, \end{aligned} \quad (30)$$

where θ refers to the scattering polar angle, $s = (k_1 + k_2)^2 = (k_3 + k_4)^2$, $c_R = \tan\theta_W$ with θ_W is the Weinberg angle, $c_L = -\cot 2\theta_W$, $s_Z = s - M_Z^2 + iM_Z\Gamma_Z$, $s_X = s - M_X^2 + iM_X\Gamma_X$, and $\alpha = e^2/4\pi$ is the fine-structure constant.

One defines the differential cross-section for purely-polarized initial state with the helicity of

the final states summed up as

$$\frac{d\sigma_{\sigma_1\sigma_2}}{d\cos\theta} = \frac{1}{32\pi s} \sum_{\sigma_3,\sigma_4} |\mathcal{M}|^2. \quad (31)$$

Then, by introducing the longitudinal polarization of the electron and positron beams, we define the partially-polarized differential cross-section as

$$\frac{d\sigma(P_{e-}, P_{e+})}{d\cos\theta} = \sum_{\sigma_1,\sigma_2} \frac{1 + \sigma_1 P_{e-}}{2} \frac{1 + \sigma_2 P_{e+}}{2} \frac{d\sigma_{\sigma_1\sigma_2}}{d\cos\theta}, \quad (32)$$

where P_{e-} and P_{e+} ($-1 \leq P_{e\pm} \leq 1$) are the polarization degrees of the electron and positron beams, respectively, which the electron (positron) beams are purely right-handed polarized when $P_{e-} = 1$ ($P_{e+} = 1$). Using the realistic values at the ILC [58], we define the polarized differential cross-sections as

$$\frac{d\sigma_R}{d\cos\theta} \equiv \frac{d\sigma(0.8, -0.3)}{d\cos\theta}, \quad \frac{d\sigma_L}{d\cos\theta} \equiv \frac{d\sigma(-0.8, 0.3)}{d\cos\theta}. \quad (33)$$

The forward-backward asymmetry associated with the polarized cross-section $\sigma_L(\sigma_R)$ is determined by the following quantity

$$A_{FB}^{L(R)} = \frac{N_F^{L(R)} - N_B^{L(R)}}{N_F^{L(R)} + N_B^{L(R)}}, \quad (34)$$

where

$$N_{F(B)}^i = \epsilon \mathcal{L} \int_{0(-c_{\max})}^{c_{\max}(0)} d\cos\theta \frac{d\sigma_i}{d\cos\theta}, \quad (35)$$

with i referring to L or R , ϵ to be the efficiency of observing the events which are equal to one for electron and muon final states, $c_{\max} = 0.95$ for the muon final state [59]. We estimate the sensitivity to the contribution of the X gauge boson to FB asymmetry of the process $e^+e^- \rightarrow \mu^+\mu^-$ by the following quantity

$$\Delta A_{FB}^{L(R)} = \left| A_{FB}^{L(R)} \Big|_{\text{SM}+X} - A_{FB}^{L(R)} \Big|_{\text{SM}} \right|, \quad (36)$$

where $A_{FB}^{L(R)} \Big|_{\text{SM}}$ and $A_{FB}^{L(R)} \Big|_{\text{SM}+X}$ refer to FB asymmetry for the cases coming from only the SM boson contribution and from the SM plus X boson contributions. This quantity should be compared with the statistical error of FB asymmetry which we assume from the SM boson contribution only, given by [60, 61]

$$\delta A_{FB}^{L(R)} = \sqrt{\frac{1 - \left(A_{FB}^{L(R)} \Big|_{\text{SM}} \right)^2}{N_F^{L(R)} \Big|_{\text{SM}} + N_B^{L(R)} \Big|_{\text{SM}}}}. \quad (37)$$

We require $\Delta A_{FB}^{L(R)} > 2\sigma$ for which the signal of the X gauge boson could manifest itself over the SM background.

In Fig. 2, we show the sensitivity to the contribution of the X gauge boson in FB asymmetry of the process $e^+e^- \rightarrow \mu^+\mu^-$ as a function of $M_X R$, for the polarized cross-sections $\sigma_{R,L}$ and various integrated luminosities, at the center of mass energy $\sqrt{s} = 500$ GeV. Furthermore, we have included the predictions of FB asymmetry from the $U(1)_{B-L}$ model [11, 12] and the $U(1)_R$ model [41] for comparison. From this figure, we find that the regions $M_X R \lesssim 7.31(8.8) \times 10^{-15}$

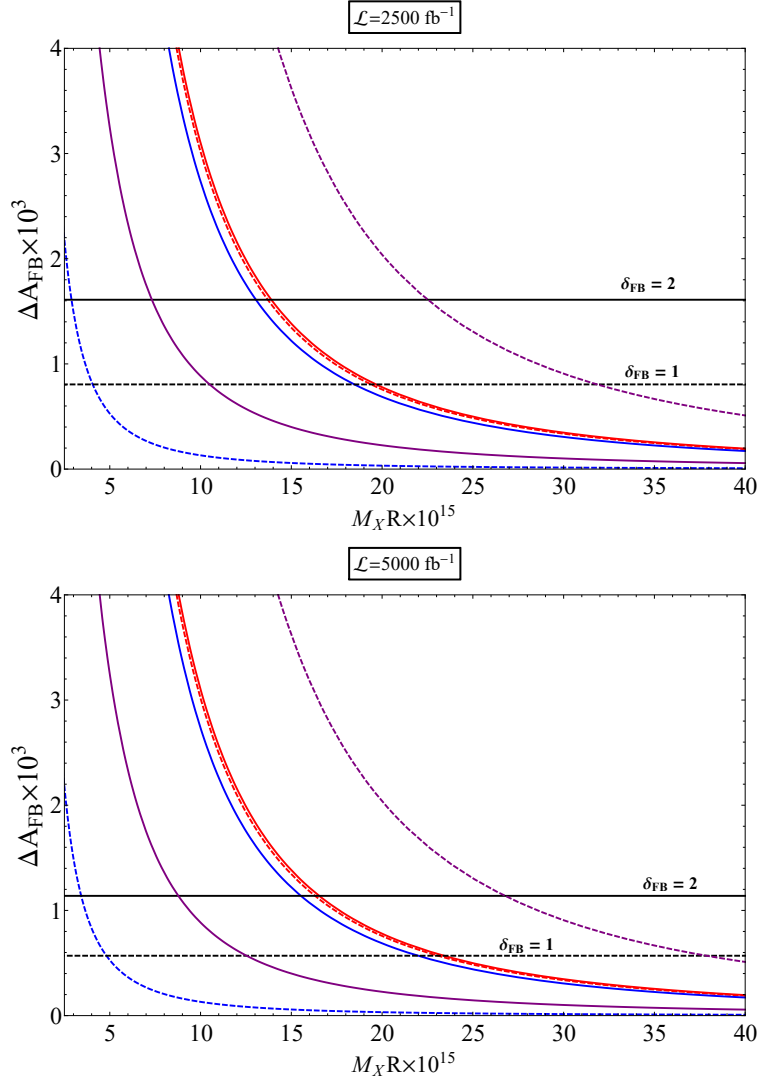


FIG. 2: The quantity $\Delta A_{FB}^{L(R)}$, describing the contribution of the new neutral gauge boson to FB asymmetry for the process $e^+e^- \rightarrow \mu^+\mu^-$ at the ILC, as a function of $M_X R$. The solid and dashed curves correspond to the polarized cross-sections σ_R and σ_L , respectively. The purple, red, and blue curves correspond to our model, $U(1)_{B-L}$ model, and $U(1)_R$ model, respectively. The dashed and solid black horizontal lines refer to the 1σ and 2σ confidence levels, respectively.

and $M_X R \lesssim 22.46(26.8) \times 10^{-15}$ can give more 2σ sensitivity to the contribution of the X gauge boson in FB asymmetry of the final-state mode $\mu^+\mu^-$ for the polarized cross-sections σ_R and σ_L , respectively, at integrated luminosity $\mathcal{L} = 2500(5000) \text{ fb}^{-1}$. However, with the mass of the X gauge boson below 5.5 TeV, the more 2σ sensitive region for the polarized cross-section σ_R should almost be excluded by the current LHC limits on the production of new gauge boson, as indicated in Fig. 3. Only the polarized cross-section σ_L can contain the allowed parameter region giving more 2σ sensitivity after combining the current LHC limits.

It is remarkable that, by comparing the difference of ΔA_{FB} between the polarized cross-sections σ_R and σ_L , one can easily distinguish the new neutral gauge boson in our model from those predicted in the $U(1)_{B-L}$ and $U(1)_R$ models. More specifically, both our model and $U(1)_R$ model provide the significant difference between the polarized cross-sections σ_R and σ_L due to the fact that the left-handed and right-handed fermions in these models have the relatively different couplings to the new neutral gauge boson. Whereas, the $U(1)_{B-L}$ model gives the small difference between σ_R and σ_L . In addition, in our model ΔA_{FB} of the polarized cross-sections σ_L is relatively larger than that of σ_R . This happens by the contrary in the $U(1)_R$ model.

B. Left-right asymmetry

Now we analyze the left-right asymmetry of the process $e^+e^- \rightarrow \mu^+\mu^-$ which is defined by the following quantity

$$A_{LR} = \frac{N_L - N_R}{N_L + N_R}, \quad (38)$$

where N_L and N_R are the numbers of the events corresponding to the purely right-handed and right-handed polarized initial-state electron beams, respectively, which are given by

$$\begin{aligned} N_L &= \epsilon \mathcal{L} \int_{-c_{\max}}^{c_{\max}} d \cos \theta \frac{d\sigma(-1, 1)}{d \cos \theta}, \\ N_R &= \epsilon \mathcal{L} \int_{-c_{\max}}^{c_{\max}} d \cos \theta \frac{d\sigma(1, -1)}{d \cos \theta}, \end{aligned} \quad (39)$$

with $d\sigma(P_{e-}, P_{e+})/d \cos \theta$ to be given in Eq. (32). Then, we define the deviation of left-right asymmetry from the SM prediction with respect to the process $e^+e^- \rightarrow \mu^+\mu^-$ by the following quantity

$$\Delta A_{LR} = \left| A_{LR} \Big|_{\text{SM}+X} - A_{LR} \Big|_{\text{SM}} \right|, \quad (40)$$

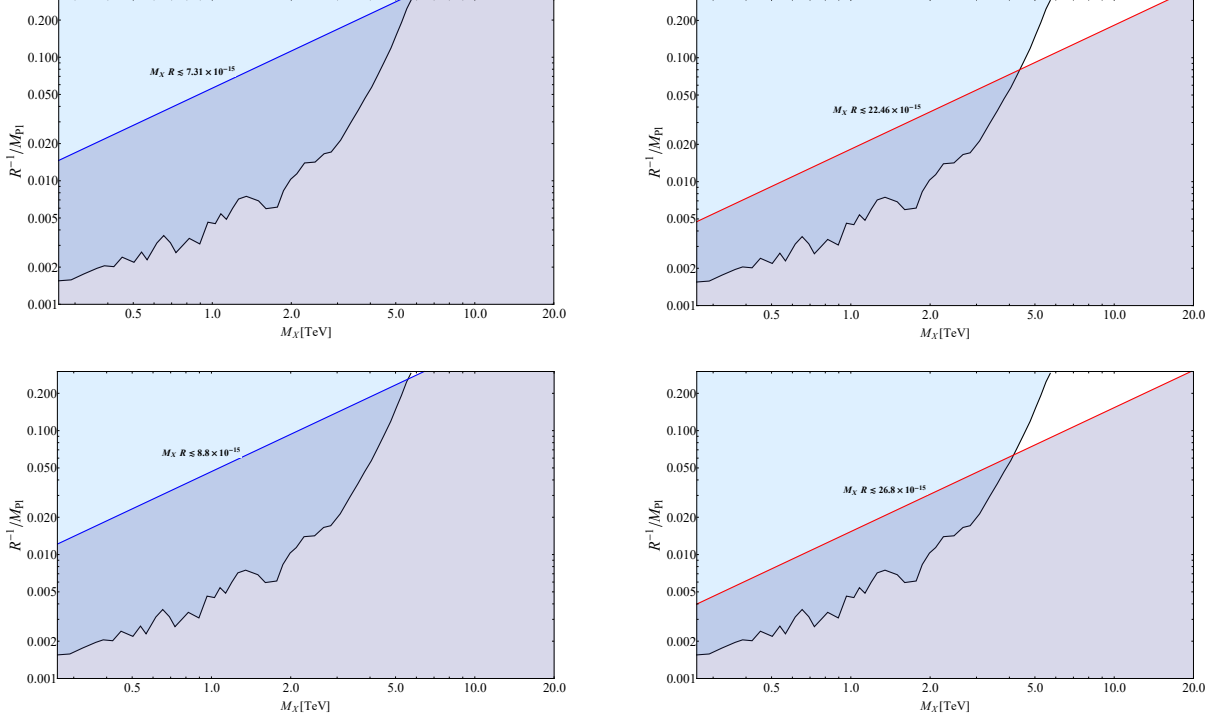


FIG. 3: The allowed parameter regions in the $M_X - R^{-1}/M_{Pl}$ plane can give more 2σ sensitivity to FB asymmetry for the process $e^+e^- \rightarrow \mu^+\mu^-$ at the ILC, referring to the white regions. The regions above the black curve are excluded by the current LHC bound, whereas the regions above the blue and red curves can give more 2σ sensitivity.

where $A_{LR}|_{SM}$ and $A_{LR}|_{SM+X}$ refer to left-right asymmetries which are predicted by the SM and our model, respectively. We compare this quantity ΔA_{LR} with the statistical error of left-right asymmetry (assuming from the SM contribution only) given as [62]

$$\delta A_{LR} = \sqrt{\frac{1 - \left(A_{LR}|_{SM}\right)^2}{N_L|_{SM} + N_R|_{SM}}}. \quad (41)$$

In Fig. 4, we present the sensitivity to the contribution of the new neutral gauge boson in the left-right asymmetry of the process $e^+e^- \rightarrow \mu^+\mu^-$ as a function of $M_X R$, coming from our model and the $U(1)_{B-L}$ and $U(1)_R$ models, at the center of mass energy $\sqrt{s} = 500$ GeV for various integrated luminosities. From this figure, one sees that the deviation of left-right asymmetry of the process $e^+e^- \rightarrow \mu^+\mu^-$ in our model is relatively large compared to the $U(1)_{B-L}$, and $U(1)_R$ models. In this sense, our model can be distinguished from the $U(1)_{B-L}$ and $U(1)_R$ models. In addition, according to this figure, we can find upper bounds for $M_X R$ which correspond to the 2σ , 4σ , and 5σ confidence levels, given in Table II. Furthermore, by combining this with the current

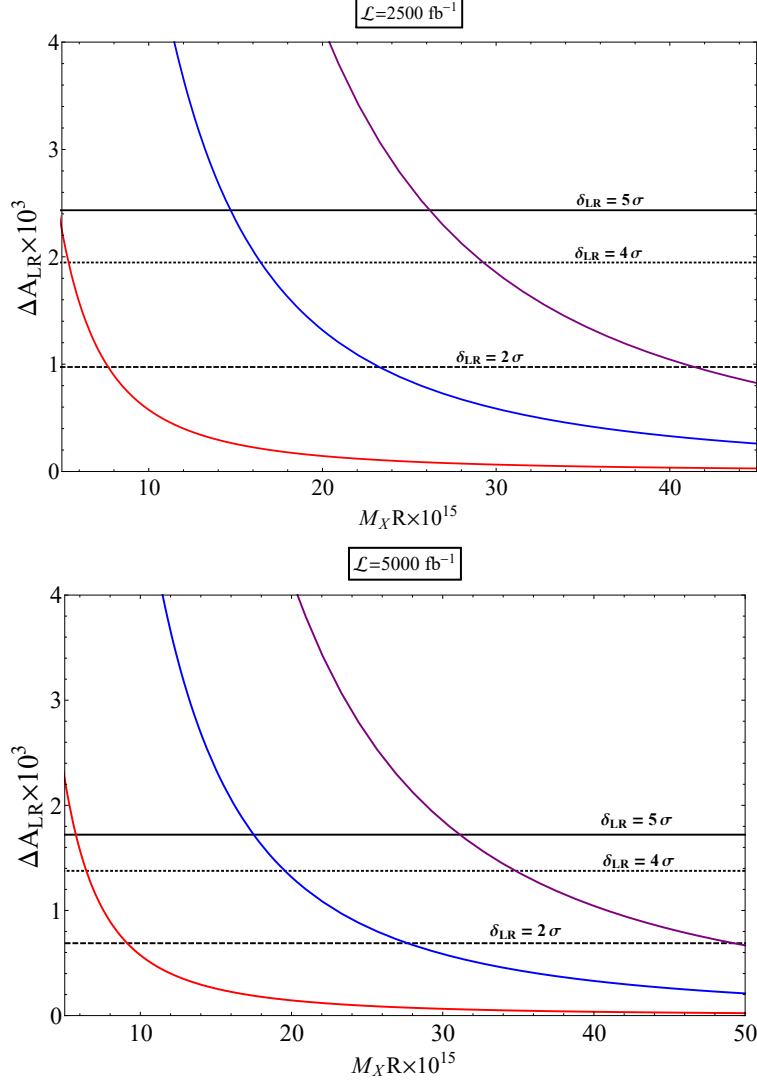


FIG. 4: The quantity ΔA_{LR} , describing the contribution of the new neutral gauge boson to left-right asymmetry for the process $e^+e^- \rightarrow \mu^+\mu^-$, as a function of $M_X R$. The purple, red, and blue curves correspond to our model, $U(1)_{B-L}$ model, and $U(1)_R$ model, respectively. The dashed, dotted, and solid black horizontal lines refer to the 2σ , 4σ , and 5σ confidence levels, respectively.

	$\mathcal{L} = 2500 \text{ fb}^{-1}$	$\mathcal{L} = 5000 \text{ fb}^{-1}$
$> 2\sigma$	$M_X R \lesssim 41.38 \times 10^{-15} \text{ TeV}$	$M_X R \lesssim 49.52 \times 10^{-15}$
$\geq 4\sigma$	$M_X R \lesssim 29.3 \times 10^{-15}$	$M_X R \lesssim 34.76 \times 10^{-15}$
$\geq 5\sigma$	$M_X R \lesssim 26.2 \times 10^{-15}$	$M_X R \lesssim 31.1 \times 10^{-15}$

TABLE II: The regions, obtained from Fig. 4, can give the $> 2\sigma$ sensitivity, $\geq 4\sigma$ sensitivity, and discovery reach at $\geq 5\sigma$ statistical significance for various values of integrated luminosity.

LHC limits on the production of the new gauge boson, we can find the allowed parameter regions in the $M_X - R^{-1}/M_{\text{Pl}}$ plane which can give to the $> 2\sigma$, $\geq 4\sigma$, and $\geq 5\sigma$ confidence levels in probing for the signal of the X gauge boson, shown in Fig. 5. From this figure, we find that the

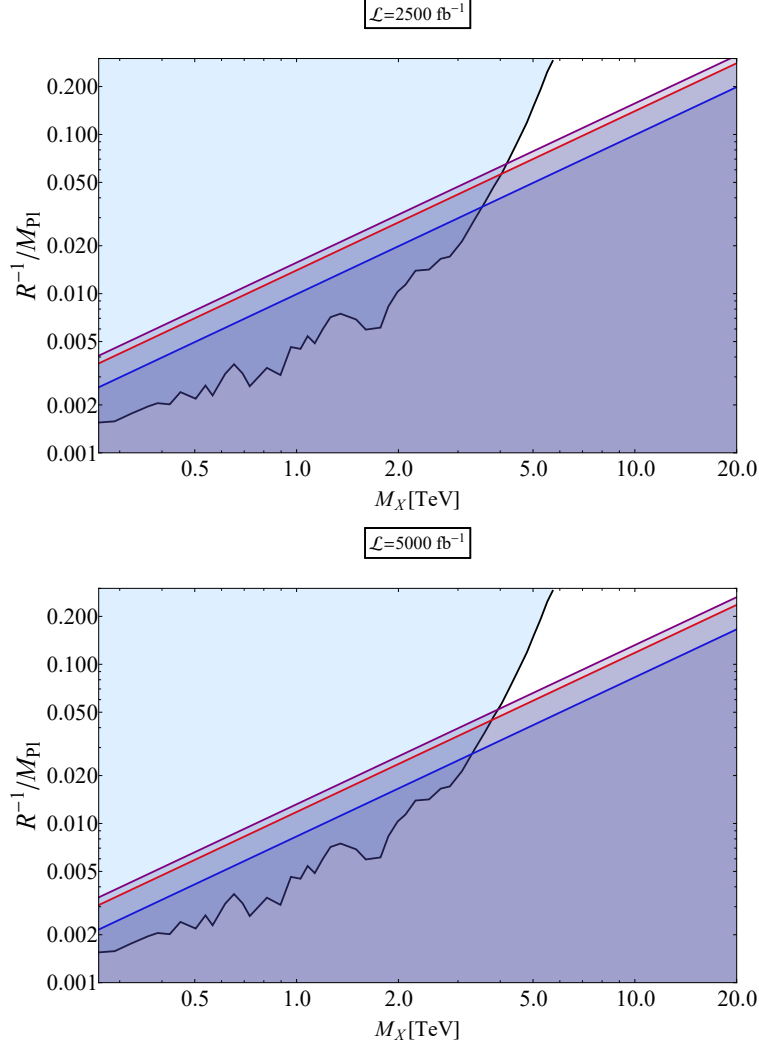


FIG. 5: The regions above the black curve are excluded by the current LHC bound, whereas the regions above the blue, red, and purple curves can give the $> 2\sigma$, $> 4\sigma$, and $> 5\sigma$ confidence levels, respectively.

allowed parameter region of the $> 2\sigma$ sensitivity with respect to left-right asymmetry is larger than that of FB asymmetry. Also, it includes the relatively significant allowed parameter regions which can achieve the discovery of $\geq 5\sigma$ statistical significance.

C. Mixed left-right-forward-backward asymmetry

Finally, we study LRFB asymmetry of the process $e^+e^- \rightarrow \mu^+\mu^-$ which is defined by the following quantity

$$A_{LRFB} = \frac{(N_F - N_B)_L - (N_F - N_B)_R}{(N_F + N_B)_L + (N_F + N_B)_R}, \quad (42)$$

where

$$\begin{aligned} (N_F - N_B)_L &= \epsilon \mathcal{L} \left[\int_0^{c_{\max}} d \cos \theta \frac{d\sigma(-1, 1)}{d \cos \theta} - \int_{-c_{\max}}^0 d \cos \theta \frac{d\sigma(-1, 1)}{d \cos \theta} \right], \\ (N_F - N_B)_R &= \epsilon \mathcal{L} \left[\int_0^{c_{\max}} d \cos \theta \frac{d\sigma(1, -1)}{d \cos \theta} - \int_{-c_{\max}}^0 d \cos \theta \frac{d\sigma(1, -1)}{d \cos \theta} \right]. \end{aligned} \quad (43)$$

Similarly, we show the deviation of LRFB asymmetry from the SM prediction for the process $e^+e^- \rightarrow \mu^+\mu^-$ in our model and the $U(1)_{B-L}$, and $U(1)_R$ models in Fig. 6. From this figure, we see that the qualitative behavior of LRFB asymmetry is similar to the behavior of left-right asymmetry. But, only upper values for $M_X R$ corresponding to the 2σ , 4σ , and 5σ confidence levels are smaller than those of left-right asymmetry.

V. CONCLUSION

An additional $U(1)$ gauge symmetry corresponding to a new neutral gauge boson provides a minimal extension of the Standard Model (SM) and it is an active area at the LHC and future colliders such as the International Linear Collider (ILC). In traditional way, the additional $U(1)$ gauge symmetry is introduced through extending the $SU(3)_C \times SU(2)_L \times U(1)_Y$ gauge symmetry of the SM. However, the additional $U(1)$ gauge symmetry may be emerged in the effective four-dimensional spacetime from the more fundamental five-dimensional spacetime which has a topologically nontrivial structure, as proposed in our recent works [45, 46]. On the other hand, such an additional $U(1)$ gauge symmetry is actually not fundamental but emergent.

After reviewing the emergent $U(1)$ extension of SM, we have studied the phenomenology of the corresponding neutral gauge boson at colliders, focusing on its couplings to the SM fermions. Using the LEP bound and 13 TeV LHC data with 140 fb^{-1} luminosity, we have imposed the constraints on the mass and gauge coupling of the new gauge boson at which the current LHC data leads to the most stringent constraint. In addition, we have analyzed forward-backward, left-right, and left-right-forward-backward asymmetries of the process $e^+e^- \rightarrow \mu^+\mu^-$ at which we have shown

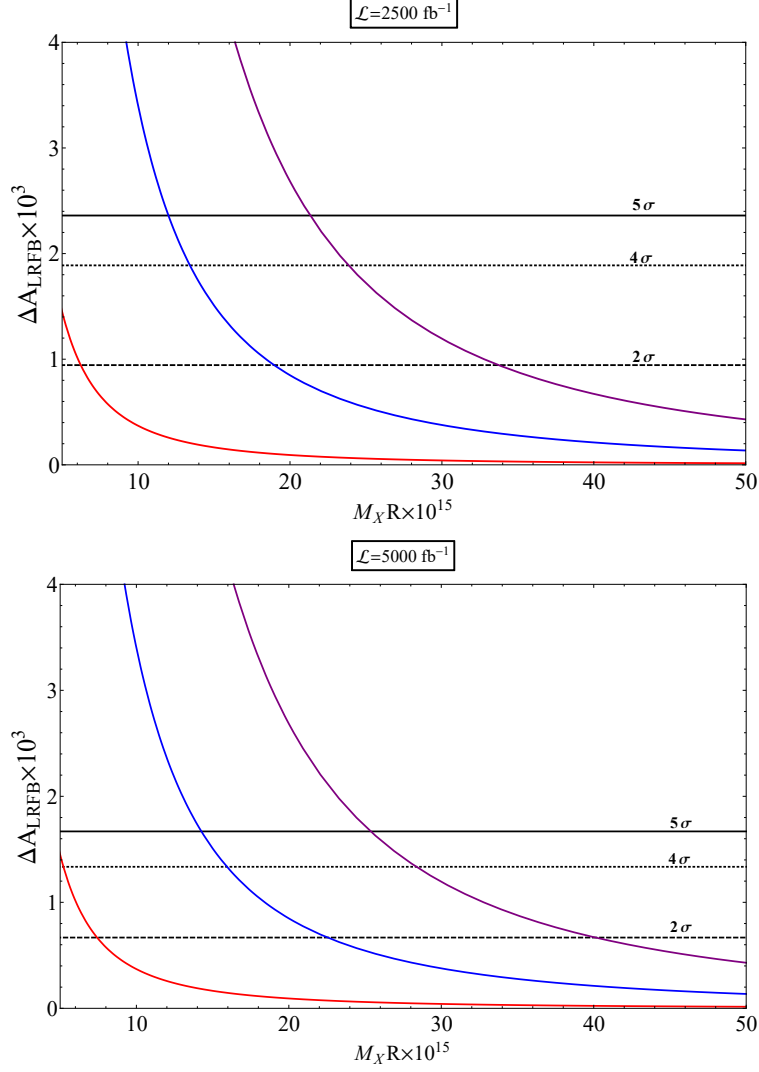


FIG. 6: The quantity, describing the contribution of the new neutral gauge boson to LRFB asymmetry for the process $e^+e^- \rightarrow \mu^+\mu^-$, as a function of $M_X R$. The purple, red, and blue curves correspond to our model, $U(1)_{B-L}$ model, and $U(1)_R$ model, respectively.

that the emergent $U(1)$ extension of SM can be tested for the sufficient integrated luminosity and it can be distinguished from other models such as $U(1)_{B-L}$ and $U(1)_R$ models.

-
- [1] Y. Fukuda *et al.*, (Super-Kamiokande Collaboration), Phys. Lett. B **433**, 9 (1998).
 - [2] Y. Fukuda *et al.*, (Super-Kamiokande Collaboration), Phys. Lett. B **436**, 33 (1998).
 - [3] Y. Fukuda *et al.*, (Super-Kamiokande Collaboration), Phys. Rev. Lett. **81**, 1562 (1998).
 - [4] G. Aad *et al.* (ATLAS Collaboration), JHEP **1211** (2012) 138.
 - [5] S. Chatrchyan *et al.* (CMS Collaboration), Phys. Lett. B **720**, 63 (2013).

- [6] G. Aad *et al.* (ATLAS Collaboration), Phys. Rev. D **90**, 052005 (2014).
- [7] V. Khachatryan *et al.* (CMS Collaboration), JHEP **1504** (2015) 025.
- [8] M. Aaboud *et al.* (ATLAS Collaboration), Phys. Lett. B **761**, 372 (2016).
- [9] M. Aaboud *et al.* (ATLAS Collaboration), JHEP **1710** (2017) 182.
- [10] V. Khachatryan *et al.* (CMS Collaboration), Phys. Lett. B **768**, 57 (2017).
- [11] R. N. Mohapatra and R. E. Marshak, Phys. Rev. Lett. **44**, 1316 (1980); **44**, 1643(E) (1980).
- [12] R. E. Marshak and R. N. Mohapatra, Phys. Lett. **91B**, 222 (1980).
- [13] S. Khalil, J. Phys. G **35**, 055001 (2008).
- [14] S. Iso, N. Okada, and Y. Orikasa, Phys. Lett. B **676**, 81 (2009).
- [15] S. Khalil, Phys. Rev. D **82**, 077702 (2010).
- [16] A. Latosinski, K. A. Meissner, and H. Nicolai, Eur. Phys. J. C **73**, 2336 (2013).
- [17] A. Das, N. Okada, and N. Papapietro, Eur. Phys. J. C **77**, 122 (2017).
- [18] A. Biswas, S. Choubey, and S. Khan, Eur. Phys. J. C **77**, 875 (2017).
- [19] S. Singirala, R. Mohanta, and S. Patra, Eur. Phys. J. Plus **133**, 477 (2018).
- [20] T. Nomura, Eur. Phys. J. C **78**, 189 (2018).
- [21] D. A. Camargo, M. D. Campos, T. B. de Melo, and F. S. Queiroz, Phys. Lett. B **795**, 319 (2019).
- [22] C. Marzo, L. Marzola, and V. Vaskonen, Eur. Phys. J. C **79**, 601 (2019).
- [23] W. Chao, Phys. Lett. B **695**, 157 (2011).
- [24] W. Chao, Phys. Rev. D **93**, 115013 (2016).
- [25] X. He, G. C. Joshi, H. Lew, and R. Volkas, Phys. Rev. D **43**, R22 (1991).
- [26] S. Baek, N. G. Deshpande, X.-G. He, and P. Ko, Phys. Rev. D **64**, 055006 (2001).
- [27] J. Heeck and W. Rodejohann, Phys. Rev. D **84**, 075007 (2011).
- [28] W. Altmannshofer, S. Gori, M. Pospelov, and I. Yavin, Phys. Rev. D **89**, (2014) 095033.
- [29] M. Das and S. Mohanty, Phys. Rev. D **89**, 025004 (2014).
- [30] S. Baek, H. Okada, and K. Yagyu, JHEP **1504** (2015) 049.
- [31] A. Biswas, S. Choubey, and S. Khan, JHEP **1609** (2016) 147.
- [32] K. Asai, K. Hamaguchi and N. Nagata, Eur. Phys. J. C **77**, 763 (2017).
- [33] S. Lee, T. Nomura, and H. Okada, Nucl. Phys. B **931**, 179 (2018)
- [34] A. Kamada, K. Kaneta, K. Yanagi, and H. B. Yu, JHEP **1806** (2018) 117.
- [35] G. Arcadi, T. Hugle, and F. S. Queiroz, Phys. Lett. B **784**, 151 (2018).
- [36] H. Banerjee, P. Byakti, and S. Roy, Phys. Rev. D **98**, 075022 (2018).
- [37] J.-X. Hou and C.-X. Yue, Eur. Phys. J. C **79**, 983 (2019).
- [38] T. Nomura and H. Okada, Phys. Lett. B **761**, 190 (2016).
- [39] T. Nomura and H. Okada, Phys. Rev. D **96**, 015016 (2017).
- [40] M. D. Campos, D. Cogollo, M. Lindner, T. Melo, F. S. Queiroz, and W. Rodejohann, JHEP **1708** (2017) 092.
- [41] T. Nomura and H. Okada, Phys. Rev. D **97**, 015015 (2018).

- [42] W. Chao, Eur. Phys. J. C **78**, 103 (2018).
- [43] S. Jana, P. K. Vishnu, and S. Saad, Eur. Phys. J. C **79**, 916 (2019).
- [44] C. H. Nam, J. Phys. G **48**, 015004 (2020).
- [45] C. H. Nam, Eur. Phys. J. C **79**, 384 (2019).
- [46] C. H. Nam, Eur. Phys. J. C **80**, 231 (2020).
- [47] T. Kaluza, Sitzungsber. Preuss. Akad. Wiss. Berlin (Math. Phys.) 1921: 966972 (1921).
- [48] O. Klein, Zeitschrift fr Physik a Hadrons and Nuclei 37 (12): 895906 doi:10.1007/BF01397481 (1926).
- [49] D. Bailin and A. Love, Rep. Prog. Phys. **50**, 1087 (1987).
- [50] J. M. Overduin and P. S. Wesson, Phys. Rep. **283**, 303 (1997).
- [51] Mikio Nakahara, *Geometry, Topology and Physics*, Institute of Physics Publishing, London (2003).
- [52] S. Schael *et al.* (ALEPH and DELPHI and L3 and OPAL and LEP Electroweak Collaborations), Phys. Rep. **532**, 119 (2013).
- [53] E. Accomando, A. Belyaev, J. Fiaschi, K. Mimasu, S. Moretti, and C. Shepherd-Themistocleous, JHEP **1601** (2016) 127.
- [54] A. D. Martin, W. J. Stirling, R. S. Thorne and G. Watt, Eur. Phys. J. C **63**, 189 (2009).
- [55] CMS Collaboration, *Search for a narrow resonance in high-mass dilepton final states in proton-proton collisions using 140 fb^{-1} of data at $\sqrt{s} = 13\text{ TeV}$* , CMS-PAS-EXO-19-019.
- [56] CMS collaboration, A. M. Sirunyan *et al.*, JHEP **07** (2021) 208.
- [57] W. Abdallah, J. Fiaschi, S. Khalil, and S. Moretti, JHEP **1602** (2016) 157.
- [58] H. Baer *et al.*, *The International Linear Collider technical design report - Volume 2: physics*, arXiv: 1306.6352.
- [59] T. H. Tran, V. Balagura, V. Boudry, J.-C. Brient, and H. Videau, Eur. Phys. J. C **76**, 468 (2016).
- [60] A. Djouadi, A. Leike, T. Riemann, D. Schaile, and C. Verzegnassi, Z. Phys. C **56**, 289 (1992).
- [61] T. Nomura and H. Okada, JHEP **1801** (2018) 099.
- [62] A. Leike and S. Riemann, Z. Phys. C **75**, 341 (1997).